of intramolecular electron transfer from the nitrogen center.

Experimental Section

The 2-aryl-3-benzoyl- and 2,3-dibenzoylaziridines employed in the present study were prepared through the reaction of appropriate amines with requisite α,β-dibromoketones. Procedures reported in the literature were followed. Melting points and references are as follows: **1** (99–100 °C);[26,27] **2a** (101–102 °C);[26,27] **2b** (105–106 °C);[27-29] **3** (90–91 °C);[30,31] **4** (122 °C);[32] **5** (124–125 °C);[32] **6a** (138–139 °C);[27,33] **6b** (149–150 °C);[27,33] and **7** (135–136 °C).[27,33] Stereochemical assignments of both cis and trans isomers were confirmed by ^{1}H NMR spectra[33,34] recorded on a Nicolet NB-300 NMR spectrometer. The solvents employed were Aldrich Gold Label benzene, methanol, and acetonitrile. MN, DMHD, and DMAD, all from Aldrich, were vacuum-distilled. Trifluoroacetic acid (Aldrich) was used as received; paraquat (methylviologen, Aldrich) was precipitated from aqueous methanol by adding excess acetone.

The absorption spectra were recorded on a Cary 219 spectrophotometer (1-nm band pass). The low-temperature ylide spectra were measured in quartz cells (3-mm-path lengths) immersed in liquid nitrogen contained in a Dewar provided with flat-faced quartz windows. The steady-state irradiation was carried out at 366, 335, or 315 nm by using the output from a medium-pressure Hg lamp (B & L SP-200) coupled with a monochromater (B & L 33-86-07).

For laser flash photolysis, pulse excitation was carried out mostly at 337.1 nm (2–3 mJ, ~8 ns), employing a Molectron UV-400 nitrogen laser system. For some experiments, the output (third harmonic, 355 nm, 5–20 mJ, 6 ns) from a Quanta-Ray Nd-YAG system was also used. The transient phenomena were observed in terms of absorption in 2–3-mm quartz cells by using a kinetic spectrophotometer described in earlier papers.[35] Unless oxygen effects were meant to be studied, the solutions were deoxygenated by purging with argon or nitrogen. In the experiments requiring a large number of laser shots (e.g., for wavelength-by-wavelength measurements of transient absorption spectra), a flow system was used in which the solution for photolysis was allowed to drain from a reservoir through the cell.

For pulse radiolysis, 5-ns electron pulses from the Notre Dame 7-MeV ARCO LP-7 linear accelerator was used at dose rates of 2×10^{16} eV/g per pulse. The details of the computer-controlled spectrophotometric detection system are available elsewhere.[36] Nitrogen-saturated benzene solutions were allowed to flow through a quartz cell (1-cm-path length) that was irradiated with electron pulses in a right-angle geometry with respect to the analyzing light. The conventional lamp flash photolysis system is described elsewhere.[37]

Acknowledgment. We are thankful to Dr. G. Ferraudi for access to the lamp flash photolysis system and to Dr. S. Das for assistance in using it.

(27) Kumar, C. V.; Ramaiah, D.; Das, P. K.; George, M. V. *J. Org. Chem.* **1985**, *50*, 2818–2825.
(28) Southwick, P. L.; Christman, D. R. *J. Am. Chem. Soc.* **1952**, *74*, 1886–1891.
(29) Bhat, V.; George, M. V. *Tetrahetron Lett.* **1977**, 4133–4136.
(30) Cromwell, N. H.; Babson, R. D.; Harris, C. E. *J. Am. Chem. Soc.* **1943**, *65*, 312–315.
(31) Cromwell, N. H.; Barker, N. G.; Wankel, R. A.; Vanderhorst, P. J.; Olson, F. W.; Anglin, J. H., Jr. *J. Am. Chem. Soc.* **1951**, *73*, 1044–1051.
(32) Cromwell, N. H.; Bamburry, R. E.; Adelfang, J. L. *J. Am. Chem. Soc.* **1960**, *82*, 4241–4245.
(33) Cromwell, N. H.; Cahoy, R. P.; Franklin, W. E.; Mercer, G. D. *J. Am. Chem. Soc.* **1957**, *79*, 922–926.
(34) Matsumoto, K.; Nakamura, S. *Heterocycles* **1980**, *14*, 837–846.
(35) Turner, A. B.; Heine, H. W.; Irving, J.; Bush, J. B., Jr. *J. Am. Chem. Soc.* **1965**, *87*, 1050–1055.
(36) Nagel, D. L.; Woller, P. B.; Cromwell, N. H. *J. Org. Chem.* **1971**, *36*, 3911–3917.
(37) (a) Das, P. K.; Encinas, M. V.; Small, R. D., Jr.; Scaiano, J. C. *J. Am. Chem. Soc.* **1979**, *101*, 6965–6970 and references therein. (b) Nagarajan, V.; Fessenden, R. W. *J. Phys. Chem.* **1985**, *89*, 2330–2335.
(38) (a) Patterson, L. K.; Lilie, J. *Int. J. Radiat. Phys. Chem.* **1974**, *6*, 129–141. (b) Schuler, R. H.; Buzzard, G. K. *Int. J. Radiat. Phys. Chem.* **1976**, *8*, 563–574. (c) Schuler, R. H. *Chem. Educ.*, submitted.
(39) Prasad, D. R.; Ferraudi, G. *Inorg. Chem.* **1983**, *22*, 1672–1674.

Recurring Chains Following Addition of Atomic Hydrogen to Acetylene

Anthony B. Callear* and Geoffrey Benedict Smith

Physical Chemistry Department, University of Cambridge, Cambridge, U.K. *(Received: October 8, 1985)*

The C_2H_3 radical was prepared by attachment of H atoms to C_2H_2. Complex chain reactions ensue: $C_2H_3 + H_2 \rightarrow C_2H_4 + H$; $C_2H_3 + C_2H_2 \rightarrow C_4H_5$; $C_4H_5 + H_2 \rightarrow C_4H_6$ (1,3-butadiene) + H; $C_4H_5 + C_2H_2 \rightarrow C_6H_6 + H$ (cis addition); $C_4H_5 + C_2H_2 \rightarrow C_6H_7$ (trans addition); $C_6H_7 + H_2 \rightarrow C_6H_8$ (*trans*-1,3,5-hexatriene) + H; $C_6H_7 + C_2H_2 \rightarrow C_8H_9$ (leading to higher members). Relative rate coefficients are derived from product ratios, and the system has been closely matched with a model scheme. The products of the mutual termination reaction of two C_2H_3 radicals have been investigated.

Introduction

The object of this research has been to characterize some reactions of the vinyl radical, C_2H_3, particularly those related to the gas chemistry in CO_2 gas cooled nuclear reactors.[1,2] C_2H_3 has been prepared by addition of H atoms to C_2H_2, which is known to be close to the high-pressure limit with a total pressure of ~500 Torr at ambient temperature. Under nearly all the conditions chosen for this work, loss of H by reactions other than addition to C_2H_2 is negligible.

There has been considerable progress in understanding aspects of the gas chemistry of C_2H_3 during the past few years. It is known that with molecular oxygen CHO and CH_2O are produced,[3] and rate coefficients have been measured.[4] Vibrationally excited products have been detected in the reactions of O and F atoms with C_2H_3.[5] Infrared emission from C_2H_3 has been observed,

(1) D. J. Norfolk, R. F. Skinner, and W. J. Williams in *Gas Chemistry in Nuclear Reactors and Large Industrial Plant*, A. Dyer, Ed., Heyden, London, 1980.
(2) D. J. Norfolk, R. F. Skinner, and W. J. Williams, *Radiat. Phys. Chem.*, **21**, 307 (1983).
(3) R. R. Baldwin and R. W. Walker, *Symp. (Int.) Combust.*, [*Proc.*], *18th, 1980*, 819 (1981).
(4) J.-Y. Park, M. C. Heaven, and D. Gutman, *Chem. Phys. Lett.*, **104**, 469 (1984).

0022-3654/86/2090-3229$01.50/0

following formation of the excited radical in the photolysis of C_2H_3Cl.[6] The discovery of an electronic system of C_2H_3 has been reported recently.[7]

However, it seem that there is little published data on reactions of C_2H_3 with H_2, C_2H_2, and CO, one aspect of the present study. Nor does there appear to be any literature on C_4H_5 and C_6H_7 reactions in the gas phase.

A preliminary report on this work has already been published.[8]

Experimental Section

Mixtures of H_2 and C_2H_2, in a cylindrical quartz reaction vessel of length 10 cm, were irradiated with 2537-Å resonance radiation from a low-pressure mercury discharge lamp. The lamp was air-cooled and maintained at 313 K. A mercury reservoir on the reaction vessel was held at 293 K.

The products were identified by gas chromatographic separation, using flame ionization detection.

The standard procedure was to admit a sample of irradiated gas to an evacuated U-tube, from which it could be injected directly into the column. For the hexatriene separation, the resolution was improved by holding up the sample in a cold trap of small diameter, immediately before the column entrance.

Calibration of the detector with C_2 and C_4 gases showed that the sensitivity of detection of the products (area under the traces) was proportional to both the number of C atoms in the molecule and the number of moles injected.

All materials were of research grade purity. C_2H_2 was thoroughly degassed and was further purified by distilling from a trap at 130 K. H_2 and CO were stored over reduced copper at 560 K.

Results

Vinyl radicals were prepared by generating atomic hydrogen in the presence of small pressures of C_2H_2.

$$Hg(^3P_1) + H_2 \rightarrow 2H \text{ (in part via HgH)}$$

$$H + C_2H_2 + M \rightarrow C_2H_3 + M$$

The method has the advantage of allowing several of the variables to be changed independently.

The positions of the resonance lamp and reaction vessel were adjusted to achieve a low light input of 1.8×10^{14} quanta cm^{-2} s^{-1} which was measured by determining the rate of formation of *n*-butane in the H plus C_2H_4 reaction; the quantum yield is $\simeq 0.85$ with high pressures of H_2. With the low excitation rate, HgH is expected to undergo thermal dissociation much more rapidly than its rate of reaction with other intermediates.

The following primary reaction products have been identified from their elution times through various columns: ethene, 1,3-butadiene, benzene, and *trans*-1,3,5-hexatriene. Comparatively small traces of a second C_4 species, possibly vinylacetylene, have been detected but not systematically investigated. Formation of C_6H_6 has been confirmed by mass spectrometry and NMR.

trans-C_6H_8 was identified by comparing elution times with a commercial sample which contained about 0.7 of the trans and 0.3 of the cis isomer. The trans form (bp 80–80.5 °C) appears first and can be almost completely separated from the cis isomer (bp 82–83 °C) on both squalane and diisodecyl phthalate. These observations are similar to those of Hwa et al.,[10] who have isolated each of the 1,3,5-hexatrienes. On oxydipropionitrile, the C_6H_6 (bp 78 °C) eluted last, so that each of the C_6 products could be estimated. On squalane, C_6H_6 coincides with *cis*-C_6H_8. The product of the H plus C_2H_2 reaction, which has the same retention time as *trans*-1,3,5-hexatriene on both columns, is increased relative to C_6H_6 in proportion to $[H_2]$; considering also the reaction scheme adduced later, there can be little doubt that in fact it is *trans*-C_6H_8. A reaction product with mass 80 has also been detected by mass spectrometry.

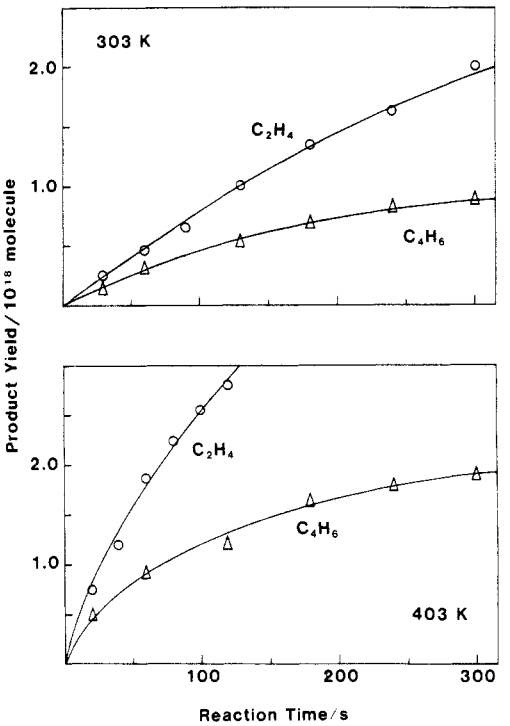

Figure 1. Formation of C_2H_4 and C_4H_6 with time: (upper) $[H_2] = 200$ Torr, $[C_2H_2] = 20$ Torr; (lower) $[H_2] = 100$ Torr, $[C_2H_2] = 8$ Torr.

A minor product occurs, $\sim 1/5$ of the *trans*-C_6H_8, having the same retention time as *cis*-C_6H_8; the yield shows little variation with either $[H_2]$ or $[C_2H_2]$. We are unable to make a definite assignment in this case, though part of this component probably is *cis*-C_6H_8, present to the extent of about 5% of the C_6H_6.

The dependence of the *trans*-C_6H_8 yields on $[H_2]$ and $[C_2H_2]$ indicated that the *trans*-C_6H_7 radical adds to C_2H_2 to form higher products; a search for higher members indicated that styrene is formed in low yield, though quantitative measurements have not been made.

In the first experiments, C_2H_4 and 1,3-C_4H_6 products were identified with an alumina column, and Figure 1 shows the evolution with time. Evidently, there is an attenuation of the rates of formation with increasing exposure; it would appear that the C_4H_6 is very susceptible to secondary attack by the reaction intermediates and rapidly attains a stationary maximum. To avoid as much as possible secondary loss of primary products, nearly all experiments at 300 K were made with a 30-s exposure, which was progressively reduced as the temperature was increased.

The initial observations seemed to indicate that these two products could result from combination and disproportionation of C_2H_3 radicals. However, examination of the effects of changing the main variables gave clear evidence of the occurrence of complex chain reactions.

(i) The C_2H_4 quantum yield is approximately proportional to $[H_2]$ for fixed $[C_2H_2]$.

(ii) All products exhibit a less than first-order dependence on light intensity, which could be varied with neutral filters. With high pressures of H_2, for each product the intensity exponents lie in the range 0.5–0.6. Those for C_2H_4 and C_4H_6 were measured for various $[H_2]$ and with $[C_2H_2]$ at 10 Torr, both at 300 and 400 K. For both, the exponents increase to ~ 0.8 as the $[H_2]$ is decreased from 700 to 50 Torr; these data are consistent with

(5) J. G. Moehlmann, J. T. Gleaves, J. W. Hudgens, and J. D. McDonald, *J. Chem. Phys.*, **60**, 4790 (1974); D. J. Donaldson and J. J. Sloan, *J. Chem. Phys.*, **77**, 4777 (1982).
(6) M. G. Moss, M. D. Ensminger, and J. D. McDonald, *J. Chem. Phys.*, **74**, 6631 (1981).
(7) H. E. Hunziker, H. Kneppe, A. D. McLean, P. Siegbahn, and H. R. Wendt, *Can. J. Chem.*, **61**, 993 (1983).
(8) A. B. Callear and G. B. Smith, *Chem. Phys. Lett.*, **105**, 119 (1984).
(9) A. B. Callear and W. P. D. Pereira, *Trans. Faraday Soc.*, **59**, 2758 (1963).
(10) J. C. H. Hwa, P. L. de Benneville, and H. J. Sims, *J. Am. Chem. Soc.*, **82**, 2537 (1960).

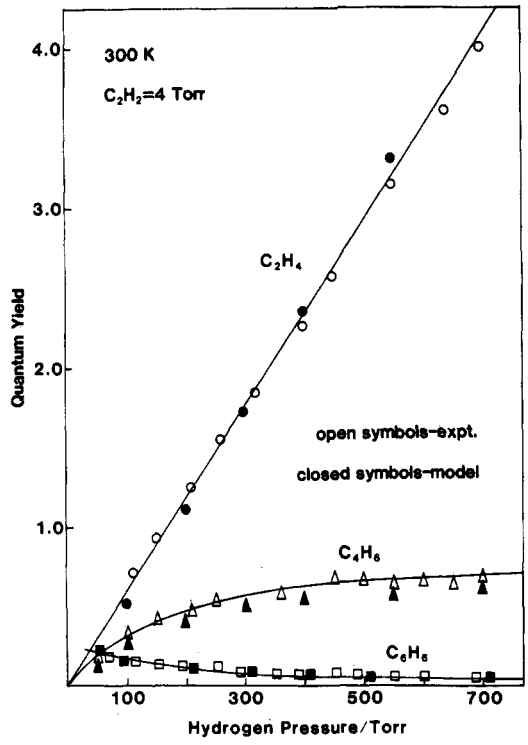

Figure 2. Product quantum yields with $[C_2H_2]$ = 4 Torr (300 K).

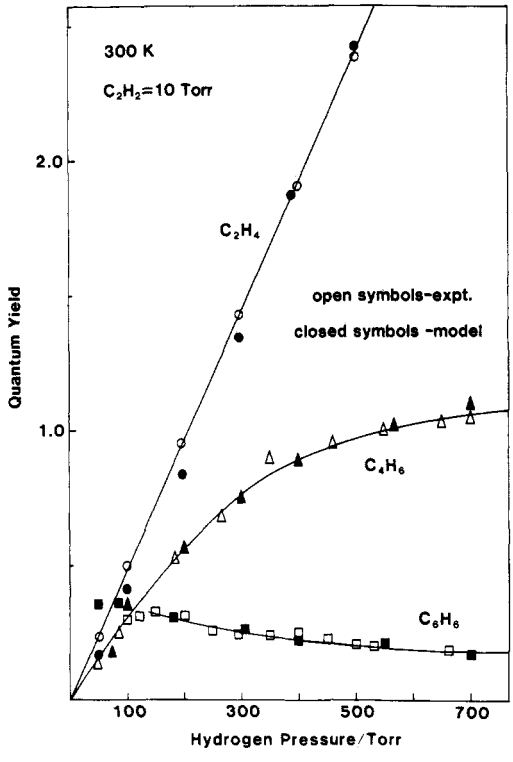

Figure 3. Product quantum yields with $[C_2H_2]$ = 10 Torr (300 K).

computation from the model reaction which is detailed later.

(iii) Formation of C_6 and higher species obviously requires a chain mechanism.

(iv) The rates of formation of all products increase approximately exponentially with increasing temperature.

The H plus C_2H_2 system is in contrast to addition of H to C_2H_4, which at low light intensities and at 300 K results solely in combination and disproportionation of C_2H_5. We have reexamined these reactions and confirm that the n-C_4H_{10} yield shows little variation with $[H_2]$ and is only slightly increased, ~5%, when the temperature is increased from 300 to 400 K. By addition of C_2H_2 to the C_2H_4/H_2 mixtures, it has also been demonstrated that no significantly addition of C_2H_5 to C_2H_2 occurs at 300 K,

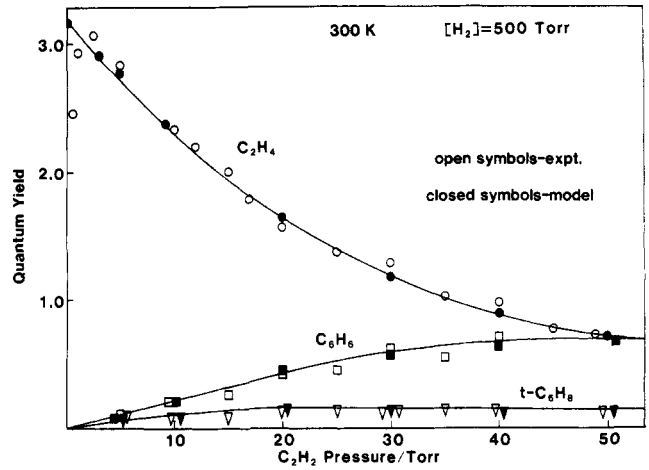

Figure 4. Product quantum yields with $[H_2]$ = 500 Torr (300 K).

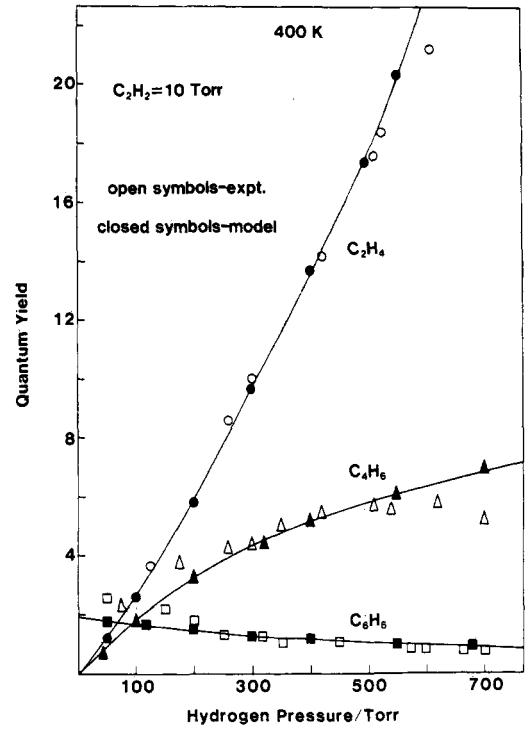

Figure 5. Product quantum yields with $[C_2H_2]$ = 10 Torr (400 K).

the yield of C_4H_{10} being unaffected by the C_2H_2 addition up to 30% of the C_2H_4.

Quantum yields for the H plus C_2H_2 reactions at 300 and 400 K are given in Figure 2–7, from both experiment and the model. Most of the quantum yields were determined for C_2H_4 formation, though a few measurements were also made for C_4H_6. The most reliable approach with regard to the results of Figure 2–7 has been to establish first the variation of $[C_2H_4]$ with both $[H_2]$ and $[C_2H_2]$, for fixed exposure. Next, product ratios were measured, first $[C_2H_4]/[C_4H_6]$ on alumina and second $[C_4H_6]/[C_6H_6]$ and $[C_6H_6]/[trans\text{-}C_6H_8]$ on diisodecyl phthalate. The quantum yields of C_4H_6 were obtained from the smoothed curve through the C_2H_4 data, and similarly the C_6H_6 yields were obtained from the smoothed C_4H_6 data.

We note the following features from the results.

(i) To within the error limits, the C_2H_4 yield, for fixed $[C_2H_2]$, is a linear function of $[H_2]$ at 300 K. However, this is not the case at 400 K, the C_2H_4 showing a slightly higher than first order dependence on $[H_2]$. The difference appears to result because a significant fraction of the C_2H_4 is formed in non chain reactions at 300 K. At the higher temperature, formation by termination is negligible, and division of the C_2H_4 yields by $[H_2]$ then gives a measure of the relative C_2H_3 concentrations.

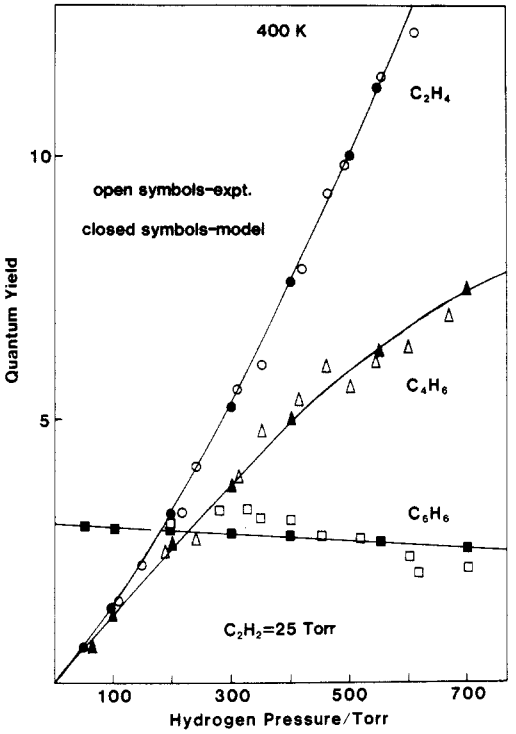

Figure 6. Product quantum yields with $[C_2H_2]$ = 25 Torr (400 K).

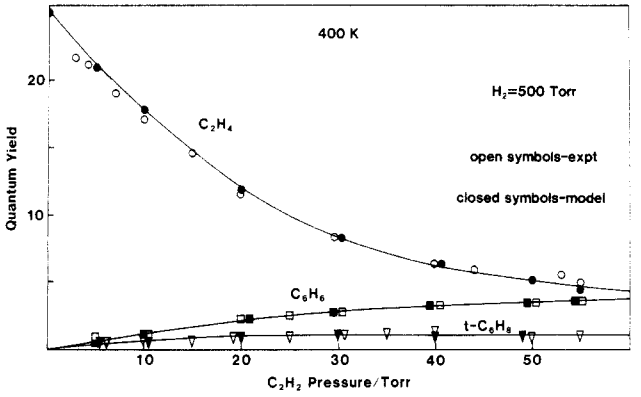

Figure 7. Product quantum yields with $[H_2]$ = 500 Torr (400 K).

(ii) The C_4H_6 increases with $[H_2]$, tending toward a limit which increases with $[C_2H_2]$.

(iii) For fixed $[C_2H_2]$, C_6H_6 increases with decreasing $[H_2]$, but for fixed $[H_2]$ C_6H_6 increases monotonically with increasing $[C_2H_2]$.

(iv) For fixed $[H_2]$, *trans*-C_6H_8 first increases with increasing $[C_2H_2]$, reaching a maximum for ~35 Torr, and decreases with further increase of $[C_2H_2]$. The *trans*-C_6H_8 quantum yields are small, and the measurements are not as reliable or as reproducible as those for the main products. It is expected to be highly reactive with respect to radical intermediates and may suffer some degree of thermal decomposition at the elevated temperatures.

Experiments have been undertaken with added N_2. With fixed $[C_2H_2]$ and various $[H_2]$, addition of N_2 to maintain the total pressure constant resulted in the same C_2H_4 quantum yields obtained without the N_2 addition. Similar experiments were carried out at 300 K to determine any total pressure dependence of the C_6H_6/*trans*-C_6H_8 ratios; no significant change of the ratios was observed on addition of excess N_2.

Considering Figures 4 and 7, the falloff of the C_2H_4 yield below about 3 Torr of C_2H_2 is probably due to the C_2H_3 plus H reaction, which regenerates C_2H_2. Four measurements of the high-pressure rate coefficient for addition of atomic hydrogen to acetylene have been reported; three groups agree on 1.5×10^{-13} cm^3 molecule^{-1} s^{-1} at 300 K,[11-14] and the other reports 3.8×10^{-13} cm^3 molecule^{-1} s^{-1} at the same temperature.[15,16] With the smaller coefficient and with C_2H_2 at 1 Torr, the mean lifetime of H is 2×10^{-4} s. We later show that the mean concentration of radicals in our experiments is $\simeq 10^{12}$ molecules cm^{-3}. Thus, if it is supposed that the rate coefficient for loss of H by reaction with C_2H_3 is 2×10^{-10} cm^3 molecule^{-1} s^{-1}, a 10% drop in the C_2H_4 yield would result with $[C_2H_2]$ at 1 Torr.

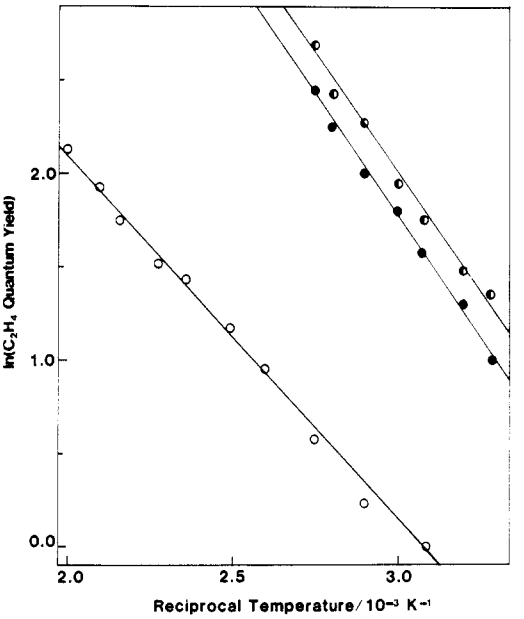

Figure 8. Arrhenius plots for the reaction of C_2H_3 with H_2: (upper set) $[C_2H_2] = 6.6 \times 10^{16}$, $[H_2] = 2 \times 10^{19}$; (middle set) $[C_2H_2] = 2.6 \times 10^{17}$, $[H_2] = 2 \times 10^{19}$; (lower set) $[C_2H_2] = 2.6 \times 10^{17}$, $[H_2] = 3.3 \times 10^{18}$ (concentrations in molecules cm^{-3}).

It is now convenient to state what is considered to be the reaction mechanism, as follows.

$$Hg(^1S_0) + h\nu \rightarrow Hg(^3P_1)$$

$$Hg(^3P_1) + H_2 \rightarrow Hg(^1S_0) + 2H$$

$$H + C_2H_2 + M \rightarrow C_2H_3 + M$$

$$C_2H_3 + H_2 \xrightarrow{k_1} C_2H_4 + H \quad (1)$$

$$C_2H_3 + C_2H_2 \xrightarrow{k_2} C_4H_5 \quad (2)$$

$$C_4H_5 + H_2 \xrightarrow{k_3} C_4H_6 + H \quad (3)$$

$$C_4H_5 + C_2H_2 \xrightarrow{k_4} C_6H_6 + H \quad (4)$$

$$C_4H_5 + C_2H_2 \xrightarrow{k_5} \textit{trans}\text{-}C_6H_7 \quad (5)$$

$$\textit{trans}\text{-}C_6H_7 + H_2 \xrightarrow{k_6} \textit{trans}\text{-}C_6H_8 + H \quad (6)$$

$$\textit{trans}\text{-}C_6H_7 + C_2H_2 \xrightarrow{k_7} C_8H_9 \text{ (leading to higher products)} \quad (7)$$

$$R_i + R_j \rightarrow \text{termination}$$

The C_4H_5 intermediate is expected to have the structure $H_2CCHCHCH$; the secondary radical would propagate branched hydrocarbon chains, which is not found; furthermore, the sec-

(11) W. A. Payne and L. J. Stief, *J. Chem. Phys.*, **64**, 1150 (1976).

(12) D. G. Keil, K. P. Lynch, J. A. Cowfer, and J. V. Michael, *Int. J. Chem. Kinet.*, **8**, 825 (1976).

(13) R. Ellul, P. Potzinger, B. Reimann, and P. Camilleri, *Ber. Bunsenges. Phys. Chem.* **85**, 407 (1981).

(14) L. B. Harding, A. F. Wagner, J. M. Bowman, G. C. Schatz, and K. Christoffel, *J. Phys. Chem.*, **86**, 4312 (1982).

(15) Y. Ishikawa, K. Sugawara, and S. Sato, *Bull. Chem. Soc. Jpn.*, **52**, 3503 (1979).

(16) K. Sugawara, K. Okazaki, and S. Sato, *Bull. Chem. Soc. Jpn.* **54**, 2872 (1981).

TABLE I: Experimental Relative Rate Coefficients and Further Details for the Model Reaction

Experimental Data

$C_2H_3 + H_2 \xrightarrow{k_1} C_2H_4 + H$
$k_1 \simeq 2.5 \times 10^{-17}$ cm^3 molecule^{-1} s^{-1} at 300 K
$\epsilon_1 = 23$ ($\pm$1.0) kJ mol^{-1}

$C_2H_3 + C_2H_2 \xrightarrow{k_2} C_4H_5$
$k_2/k_1 = 30$ (300 K); $k_2/k_1 = 24$ (400 K)

$C_4H_5 + H_2 \xrightarrow{k_3} C_4H_6 + H$
$C_4H_5 + C_2H_2 \xrightarrow{k_4} C_6H_6 + H$
$C_4H_5 + C_2H_2 \xrightarrow{k_5}$ *trans*-C_6H_7
$k_4/k_3 = 10.4$ (300 K); $k_4/k_3 = 9.2$ (400 K)
$k_5/k_3 = 11.6$ (300 K); $k_5/k_3 = 12.8$ (400 K)

trans-$C_6H_7 + H_2 \xrightarrow{k_6}$ *trans*-$C_6H_8 + H$
trans-$C_6H_7 + C_2H_2 \xrightarrow{k_7} C_8H_9$
$k_7/k_6 = 50$ (at 300 and 400 K)

Data for the Model

$k_3 = 6k_1$; $k_6 = k_1$ (at 300 and 400 K)
$T/k_1 = 5.17 \times 10^{18}$ molecules cm^{-3} (300 K)
$T/k_1 = 5.15 \times 10^{17}$ molecules cm^{-3} (400 K)

feedback of H from reaction 7:
$\gamma = 0$ (300 K); $\gamma = 0.78$ (400 K)

ondary radical, $H_2CCHCCH_2$, has a substantially lower enthalpy of formation than the primary species and would presumably not have the role of a chain carrier in this system at ambient temperatures. It would appear, therefore, that reaction 2 produces the primary 1,3-butadienyl radical with insufficient excess energy for isomerization to the secondary structure.

In the regime where $[H_2] >> [C_2H_2]$, the C_2H_3 radical is the principal intermediate, and C_2H_4 is the main product; we have attempted to obtain the activation energy of reaction 1, by measuring the C_2H_4 quantum yields, Φ, up to 500 K, with $[H_2]$ constant at 2×10^{19} molecules cm^{-3}. As the $[C_2H_2]$ is reduced, the slopes of the ln Φ vs. T^{-1} plots tend to a constant value, as shown in Figure 8. The derived activation energy for reaction 1 is 23 ($\pm$1.0) kJ mol^{-1}, listed in Table I.

Relative rate coefficients can be obtained from the experimental results by application of the stationary-state equations for the three intermediates. The rate of radical loss, T, by radical–radical termination steps will be taken to be constant for a fixed light input.

$$2\Delta I + k_3[C_4H_5][H_2] + k_6[\textit{trans}\text{-}C_6H_7][H_2] + k_7[\textit{trans}\text{-}C_6H_7][C_2H_2] = [C_2H_3](k_2[C_2H_2] + T) \quad \text{(i)}$$

$$k_2[C_2H_3][C_2H_2] = [C_4H_5](k_3[H_2] + (k_4 + k_5)[C_2H_2] + T) \quad \text{(ii)}$$

$$k_5[C_4H_5][C_2H_2] = [\textit{trans}\text{-}C_6H_7](k_6[H_2] + k_7[C_2H_2] + T) \quad \text{(iii)}$$

ΔI is the rate of light absorption per unit volume, which is treated in the model at the centroid of the radical concentration.

From (ii)

$$\frac{[C_2H_4]}{[C_4H_6]} = \frac{k_1(k_4 + k_5)}{k_2k_3} + \frac{k_1[H_2]}{k_2[C_2H_2]} + \frac{k_1T}{k_2k_3[C_2H_2]} \quad \text{(iv)}$$

and plots of $[C_2H_4]/[C_4H_6]$ are linear with $[H_2]$ for fixed $[C_2H_2]$, shown in Figure 9.

At 400 K the interpretation is reasonably straightforward, the slopes yielding $k_2/k_1 = 24$ ($\pm$2.5). A least-squares analysis yields an intercept of 0.86 for $[C_2H_2]$ at 10 Torr and 0.99 for $[C_2H_2]$ at 25 Torr. Because the C_4H_6 measurements are more reliable with the lower $[C_2H_2]$—the peaks occur well up on the C_2H_2 tail—we have settled for 0.90. The termination term is small at the high temperature, and thus we obtain $(k_4 + k_5)/k_3 = 22$.

At 300 K, a small fraction of the C_2H_4 results from disproportionation of two C_2H_3 in one of the termination steps. By applying the model, one can subtract the nonchain part due to termination with satisfactory accuracy; the residual chain part

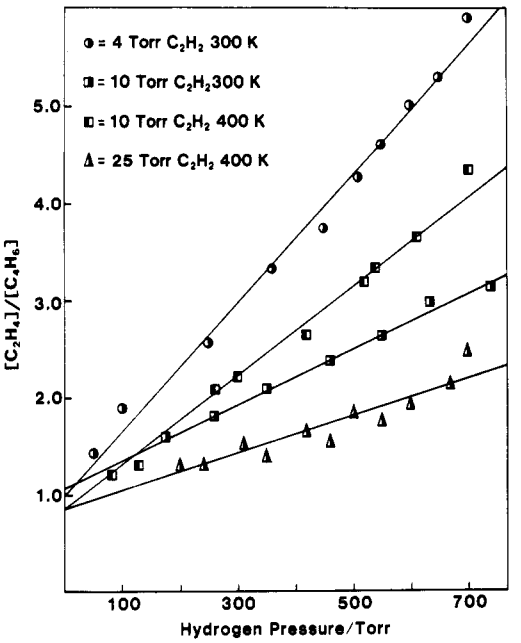

Figure 9. The $[C_2H_4]/[C_4H_6]$ ratios.

then shows a greater than first order dependence on $[H_2]$, as found directly at 400 K. And this has to be the case because, considering Figures 2, 3, 5, and 6, the vinyl radical concentration has to decrease as the $[H_2]$ is reduced. But although the termination correction can be applied to the C_2H_4, we cannot determine the total C_4H_6 which is formed by the various termination steps. We therefore take the uncorrected slopes of Figure 9 as a first approximation to k_2/k_1 at 300 K. The values so obtained are 35 with $[C_2H_2]$ at 10 Torr and 38 with $[C_2H_2]$ at 4 Torr (mean 36.5). However, the system is best modeled with a slightly lower value, $k_2/k_1 \simeq 30$, also listed in Table I.

The variation of the $[C_2H_4]/[C_4H_6]$ ratios with $[H_2]$ is similar at 300 K to that at 400 K; zero $[H_2]$ intercepts are both close to unity, indicating that the termination term

$$\frac{k_1T}{k_2k_3[C_2H_2]}$$

is small and that $k_2/k_1 \simeq (k_4 + k_5)/k_3$ at both temperatures. In order that the termination term be sufficiently small at 300 K, we have to propose that C_4H_5 is even more reactive than C_2H_3, and in the model $k_3 = 6k_1$ is used. On this basis, $(k_4 + k_5)/k_3 = 22$, which is included in Table I. It means simply that because C_4H_5 is very reactive, only a minor fraction of its removal is by radical–radical termination.

Experimental $[C_4H_6]/[C_6H_6]$ ratios allow k_4/k_3 to be measured. According to the mechanism

$$\frac{k_3}{k_4} = \frac{[C_4H_6][C_2H_2]}{[C_6H_6][H_2]}$$

should be independent of both $[H_2]$ and $[C_2H_2]$.

These quantities are plotted against $[H_2]$ in Figure 10. At 300 K, the data with $[C_2H_2]$ at 4 Torr lie significantly below those at 10 Torr. This may be due either to systematic experimental error or to partial failure of the proposed mechanism. The yields of C_6H_6 are small with $[C_2H_2]$ at 4 Torr, and the 10-Torr data have been accepted as the better approximation, yielding $k_4/k_3 = 10.4$. Within each set there is no significant change with $[C_2H_2]/[H_2]$, which emcompasses a 17-fold variation. Considering also that the yields of *cis*-1,3,5-C_6H_8 are very small, it would appear that the cis radical, resulting from addition of C_4H_5 to C_2H_2, ring-closes to generate C_6H_6 plus H sufficiently rapidly to forbid the occurrence of any alternative pathway. Considering the ratio of k_4 to $(k_4 + k_5)$, evidently about half of the addition is cis. Schemes in which the initially formed *cis*-C_6H_7 may either ring-close or undergo collisional stabilization lead to more complex behavior than that illustrated in Figure 10.

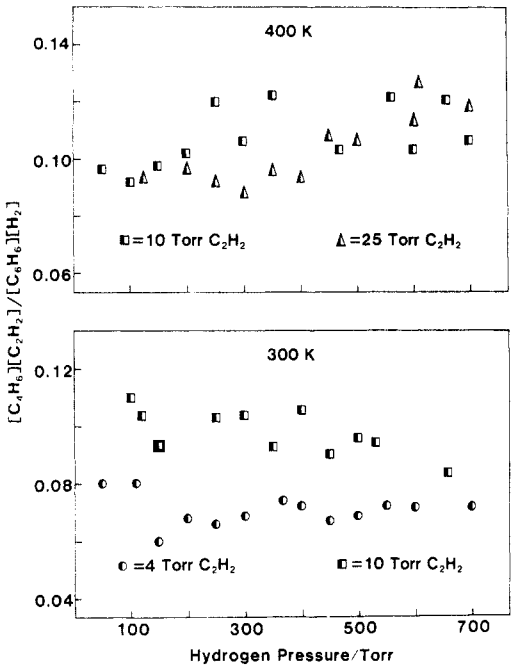

Figure 10. The quantities $[C_4H_6][C_2H_2]/[C_6H_6][H_2]$.

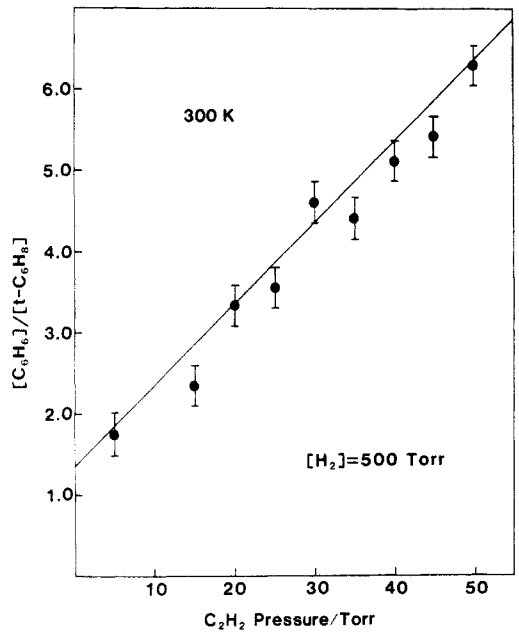

Figure 11. Variation of $[C_6H_6]/[trans\text{-}C_6H_8]$ with $[C_2H_2]$. $[H_2]$ = 500 Torr (300 K).

Similar plots for the 400 K results show that the two sets of $[C_4H_6][C_2H_2]/[C_6H_6][H_2]$ correspond well, giving $k_4/k_3 \simeq 9.2$. However, the data may possibly indicate a drift to higher values with increasing $[H_2]$, which could arise if the *trans*-C_6H_7 undergoes some degree of thermal isomerization to the cis isomer, and hence to additional C_6H_6 formation, at the higher temperature. It may be possible to achieve high conversions to C_6H_6 at even higher temperatures, if the rate of the trans-to-cis isomerization is increased.

The *trans*-C_6H_8 yields showed satisfactory reproducibility at 300 K. According to the proposed mechanism, using eq iii we should find

$$\frac{[C_6H_6]}{[C_6H_8]} = \frac{k_4}{k_5}\left(1 + \frac{k_7[C_2H_2]}{k_6[H_2]} + \frac{T}{k_6[H_2]}\right) \qquad (v)$$

The product ratios plotted vs. $[C_2H_2]$, with $[H_2]$ at 500 Torr, are given in Figure 11. We later show from the model that $T/k_6[H_2] \simeq 0.3$, which, together with $k_4/k_5 = 0.91$, predicts a zero $[C_2H_2]$ pressure intercept of $\sim$1.2. The slopes gives $k_7/k_6 = 50$ ($\pm$5) at 300 K. The same experimental data are compared to the model in Figure 4.

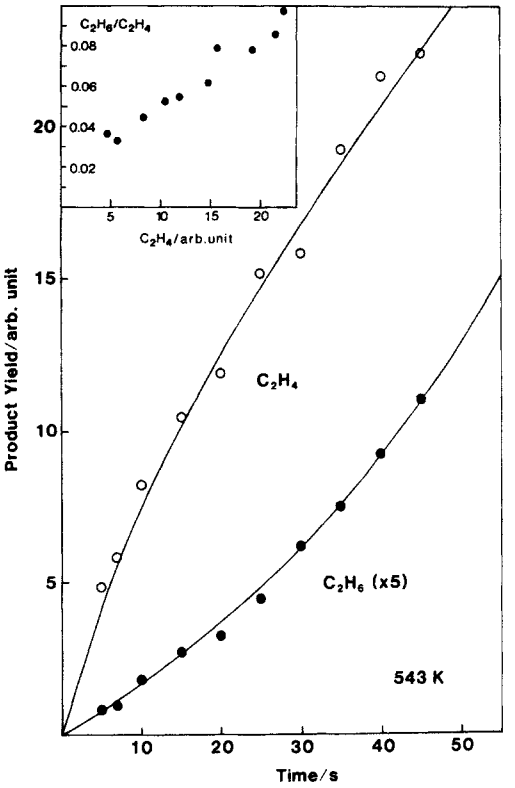

Figure 12. Time evolution of C_2H_4 and C_2H_6. The product ratio dependence on $[C_2H_4]$ is shown in the inset. The concentration units are arbitrary (543 K).

The *trans*-C_6H_8 results at 400 K are included in Figure 7 and are compared to the model by using $k_7/k_6 = 50$.

At ambient temperature the yield of C_2H_6 in the reaction is negligible with exposures up to 160 s. However, at high temperatures significant yields of C_2H_6 occur even after 10-s exposure.

Formation of C_2H_6 could result from addition of H_2 to C_2H_3 to form C_2H_5 and its disproportionation. Experiments were carried out to examine the time evolution of C_2H_6 and C_2H_4 at 543 K, and results are shown in figure 12. Even after 5 s, the rate of formation of C_2H_4 declines, while the yield of C_2H_6 exhibits a greater than first order dependence on exposure time. The $[C_2H_6]/[C_2H_4]$ ratios, given in the inset, indicates that only a very small fraction, if any, of the C_2H_6 results from addition of C_2H_3 to H_2. It is presumably produced via C_2H_5 radicals resulting from secondary addition of H to C_2H_4.

Benzene is formed in significant yield when C_2H_2 alone is subject to Hg photosensitization. We have not carried out a systematic study, and the results so far have been poorly reproducible, as if very high purity is crucial. The deactivation of $Hg(^3P_1)$ by C_2H_2 is known to excite the C_2H_2 to its first triplet state.[17]

These comments provide a review of experiments conducted with H_2/C_2H_2 mixtures, except for attempts to detect C_2H_3 termination products; the latter are deferred to the discussion because the interpretation has to be guided with a model.

One further group of experiments have been carried out to examine the behavior of the system with added CO, to determine whether or not attachment to C_2H_3 occurs. Experiments were conducted with $[H_2]/[C_2H_2]$ high, so that C_2H_3 is the predominant intermediate. We have shown that addition of CO does inhibit the rate of C_2H_4 formation over a range of temperatures. The data have been provisionally interpreted by supposing that C_2H_3

(17) C. S. Burton and H. E. Hunziker, *J. Chem. Phys.*, **57**, 339 (1972); H. E. Hunziker, H. Kneppe, A. D. McLean, P. Seigbahn, and H. R. Wendt, *Can. J. Chem.* **61**, 993 (1983).

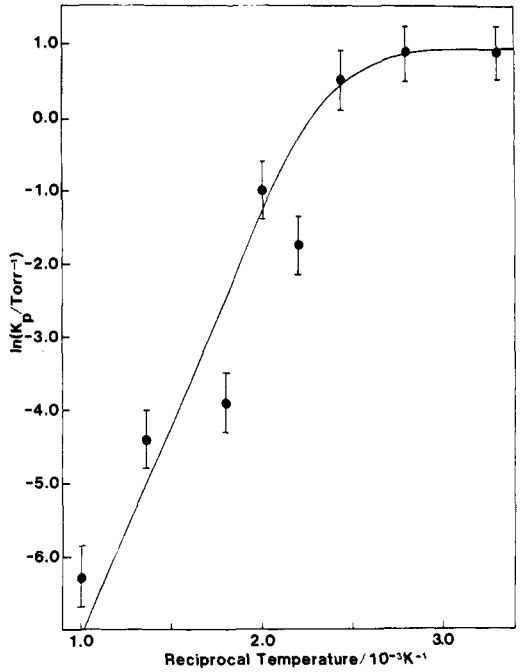

Figure 13. Temperature variation of the equilibrium constant for the reaction $C_2H_3 + CO \rightleftharpoons C_2H_3CO$.

forms an adduct with CO and that the reaction rapidly attains equilibrium.

$$C_2H_3 + CO \rightleftharpoons C_2H_3CO$$

Even at 300 K, addition of as little as 1 Torr of CO substantially decreases the C_2H_4 yields. To find the order of magnitude of the equilibrium constants, K, it is assumed that CO addition does not change the total radical concentration. Then

$$[C_2H_4]_0/[C_2H_4] = 1 + K[CO]$$

where $[C_2H_4]_0$ is the rate of C_2H_4 formation without CO addition. Such behavior was found at all temperatures, i.e., $[C_2H_4]^{-1}$ linear with [CO]; derived equilibrium constants are shown in Figure 13. The initial slow change of the equilibrium constants as the temperature is raised above 300 K suggests that in the low-temperature regime the attachment is partly rate-controlled, in which case the values obtained are lower limits. There was no significant attachment of H to CO with the conditions of these experiments.

The Model Reactions

None of the reactions described has been investigated previously, and obviously no rate coefficients are known. Hence, the model that we develop can only be a sketched outline at this stage. Nevertheless, it has proved to be of considerable interpretative and predictive value and gives unity to the various aspects.

There are two assumptions. First, it is supposed that the total radical concentration is independent of gas composition, which is equivalent to supposing that the rate coefficient for radical–radical termination is the same for all species; second, we take an exponential model for the light absorption. Neither proposition is extreme, and it has been shown already that in several applications the termination term is relatively small, so that changes in the termination rates would barely be significant. The model does not require that a numerical choice be made either of the decay constant for the exponential light absorption or for any of the rate coefficients.

The light intensity, I, after penetration to a distance x into the reaction vessel is

$$I = I_0 \exp(-\alpha x)$$

where $I_0 = 1.8 \times 10^{14}$ quanta cm^{-2} s^{-1}.

The rate of the H atom formation per unit volume at x is balanced by the termination rate.

$$2I_0\alpha \exp(-\alpha x) = k_t[R_x]^2$$

The termination coefficient is defined in terms of the radical removal rate. $[R_x]$ is the total concentration at x. Therefore

$$[R_x] = \left(\frac{2I_0\alpha}{k_t}\right)^{1/2} \exp(-\alpha x/2)$$

Upon integration it is found that

$$(R)_{total} = \left(\frac{8I_0}{\alpha k_t}\right)^{1/2}$$

while at the centroid of the radical concentration

$$[R]_{cent} = \left(\frac{I_0\alpha}{2k_t}\right)^{1/2}$$

The mean radical removal rate, T, is given by

$$T = k_t[R]_{cent} = \left(\frac{I_0\alpha k_t}{2}\right)^{1/2} = 1.34 \times 10^7 k_t^{1/2}\alpha^{1/2}\ \text{s}^{-1}$$

At 300 K and with $[H_2]$ at 500 Torr, the quantum yield for C_2H_4 formation in the $[C_2H_2] \rightarrow 0$ limit is 3.20. (The extrapolation back to $[C_2H_2] \rightarrow 0$ is actually achieved by using the model, the line being drawn through the data points of Figure 4.) Thus, with these conditions

$$\frac{k_1[H_2][R]_{total}}{2I_0} = 3.20$$

where $k_1 = 2.60 \times 10^{-12}\alpha^{1/2}k_t^{1/2}$ cm^3 molecule^{-1} s^{-1} at 300 K.

The same result is of course obtained by using the rate of light absorption at the centroid with the radical concentration at the centroid; i.e., the quantum yield at the centroid is the same as that found by integration over the x variable. Also, with regard to expressions for product ratios, such as eq iv, integration of T_x through the reaction volume yields T at the centroid, provided the integration is weighted with $[R]_x$. It is therefore an adequate approximation to develop the model at the centroid.

Thus, $T/k_1 = 5.17 \times 10^{18}$ molecules cm^{-3} at 300 K, independent of α and k_t. From the change in quantum yield of C_2H_4 formation when the temperature is increased to 400 K, we obtain $T/k_1 = 5.15 \times 10^{17}$ molecules cm^{-3} at 400 K.

To model the system, we need only the ratios of rate coefficients. For a particular radical intermediate, the required quantities have been obtained from product ratios as described. The results do not directly yield either k_1/k_3 or k_1/k_6, however. With regard to the former quantity, the only hint from experiment is the zero $[H_2]$ intercept of the $[C_2H_4]/[C_4H_6]$ ratios of Figure 9, for 300 K. These intercepts are equal to

$$\frac{k_1}{k_2}\left(\frac{k_4 + k_5}{k_3}\right) + \frac{k_1 T}{k_2 k_3[C_2H_2]}$$

and there is little change when $[C_2H_2]$ is increased from 4 to 10 Torr. If it were supposed that $k_3 = k_1$, then for 4 Torr it would be 0.52. Such behavior is not found experimentally: to match what *is* found, k_3 has to be significantly larger than k_1.

The ab initio calculations presented in ref 18 correspond to the following reaction enthalpies:

$$C_2H_3 + H_2 \rightarrow C_2H_4 + H \qquad \Delta H = -22.7\ \text{kJ mol}^{-1}$$

$$H_2CCHCHCH + H_2 \rightarrow 1,3\text{-}C_4H_6 + H \qquad \Delta H = -31.6\ \text{kJ mol}^{-1}$$

$$H_2CCHCCH_2 + H_2 \rightarrow 1,3\text{-}C_4H_6 + H \qquad \Delta H = -0.06\ \text{kJ mol}^{-1}$$

These data also indicate that $H_2CCHCHCH$ may be more reactive than C_2H_3 in respect of H abstraction from H_2. The third equation is included to support the comment made earlier that

(18) C. F. Melius, J. S. Binkley, and M. L. Koszykowski in *Proceedings of the 8th International Conference on Gas Kinetics*, Nottingham, England, 1984, Chas Goater and Son, England, 1984, p B2; C. F. Melius, private communication.

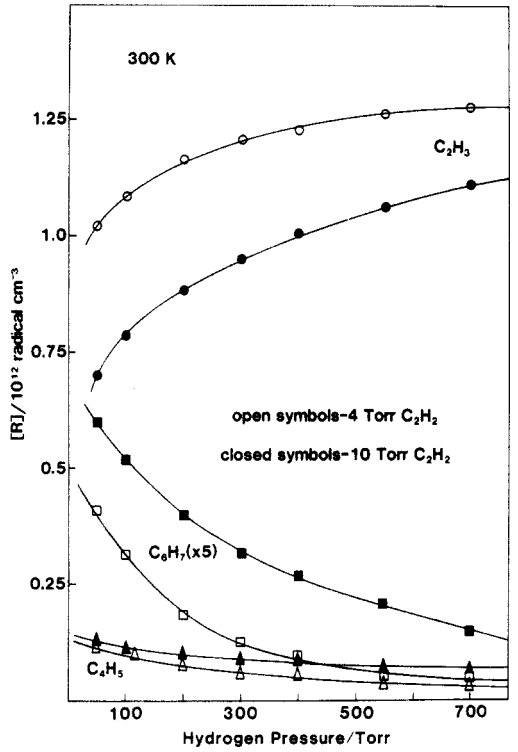

Figure 14. Radical concentrations computed from the model (all data for 300 K): ○, $[C_2H_3]$ for $[C_2H_2]$ at 4 Torr; ●, $[C_2H_3]$ for $[C_2H_2]$ at 10 Torr; △, $[C_4H_5]$ for $[C_2H_2]$ at 4 Torr; ▲, $[C_4H_5]$ for $[C_2H_2]$ at 10 Torr; □, [*trans*-C_6H_7] for $[C_2H_2]$ at 4 Torr; ■, [*trans*-C_6H_7] for $[C_2H_2]$ at 10 Torr. The *trans*-C_6H_7 concentrations have been sealed up by 5-fold.

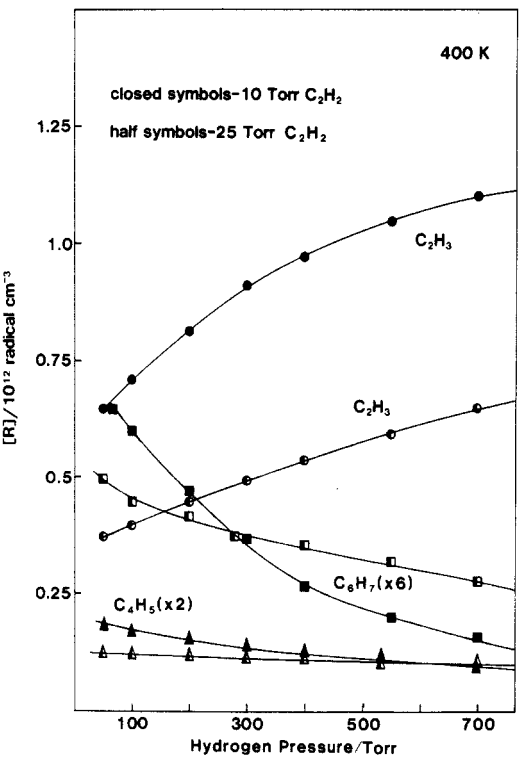

Figure 15. Radical concentrations computed from the model (all data for 400 K): ●, $[C_2H_3]$ for $[C_2H_2]$ at 10 Torr; ◐, $[C_2H_3]$ for $[C_2H_2]$ at 25 Torr; ▲, $[C_4H_5]$ for $[C_2H_2]$ at 10 Torr; ▲, $[C_4H_5]$ for $[C_2H_2]$ at 25 Torr; ■, [*trans*-C_6H_7] for $[C_2H_2]$ at 10 Torr; ◧, [*trans*-C_6H_7] for $[C_2H_2]$ at 25 Torr. The *trans*-C_6H_7 concentrations have been sealed up by 6-fold, and the C_4H_5 concentrations by 2-fold.

the secondary C_4H_5 radical is expected to be considerably less reactive than the primary. The greater stability of the secondary form has also been shown in an independent set of calculations.[19]

It has proved to be satisfactory for the model to take $k_3 = 6k_1$, both at 300 and 400 K. Referring back to Figure 9, the difference between the intercepts for the 4- and 10-Torr results (300 K) would then be 0.13, which is possible within the experimental error limits.

The choice for k_1/k_6 is less important as far as modeling the system is concerned. The addition of C_4H_5 to C_2H_2 is expected to generate the $H_2CCHCHCHCHCH$ radical. Presumably, isomerization to the structure $H_2CCHCCHCHCH_2$ does not occur signficantly, because its abstraction from H_2 would produce both *cis*- and *trans*-1,3,5-hexatriene. If k_6 is taken to equal k_1, the intercept of the Figure 10 plot is predicted to be 1.2, in accord with experiment.

The experimentally determined ratios, and the other estimates discussed in this section, are all listed in Table I.

If $[C_4H_5]$ and [*trans*-C_6H_7] are eliminated from eq i–iii, and noting that the quantum yield for formation of C_2H_4, Φ, is equal to $k_1[H_2][C_2H_3]/2\Delta I$, we obtain the following expression for Φ as a function of the concentrations.

$$\Phi^{-1} = A - B(C + D)$$

$$A = \frac{k_2[C_2H_2]}{k_1[H_2]} + \frac{T}{k_1[H_2]}$$

$$B = \frac{k_2[C_2H_2]}{k_1[H_2]}\left(1 + \frac{(k_4 + k_5)[C_2H_2]}{k_3[H_2]} + \frac{T}{k_3[H_2]}\right)^{-1}$$

$$C = 1 + \frac{k_4[C_2H_2]}{k_3[H_2]}$$

$$D = \frac{k_5[C_2H_2]}{k_3[H_2]}\left(\frac{1 + \gamma k_7[C_2H_2]/k_6[H_2]}{1 + k_7[C_2H_2]/k_6[H_2] + T/k_6[H_2]}\right)$$

(19) N. C. Handy, R. H. Nobes, and K. Somasundram, submitted for publication.

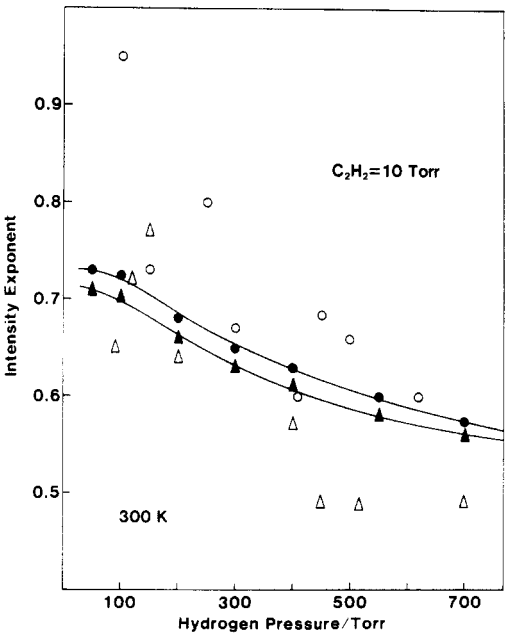

Figure 16. Intensity exponents of the C_2H_4 and C_4H_6 products (300 K): ○, C_2H_4 experiment; ●, C_2H_4 model; △, C_4H_6 experiment; ▲, C_4H_6 model.

γ is the number of H atoms which are regenerated subsequent to addition of C_6H_7 to C_2H_2.

This model was first directed at the experimental data of Figure 4, adjusting γ to fit the C_2H_4 yields with $[C_2H_2]$ at 10 and 50 Torr. In fact, with the data of Table I there are few options for variation and γ has to be set at zero. The model was then applied to predict the C_6H_6 quantum yields, and the experimental data proved to be in satisfactory agreement as shown.

By arbitrarily choosing $\alpha = 1.0$ and $k_t = 10^{-10}$ cm^3 molecule^{-1} s^{-1} (i.e., $k_1 = 2.6 \times 10^{-17}$ cm^3 molecule^{-1} s^{-1} at 300 K) we have

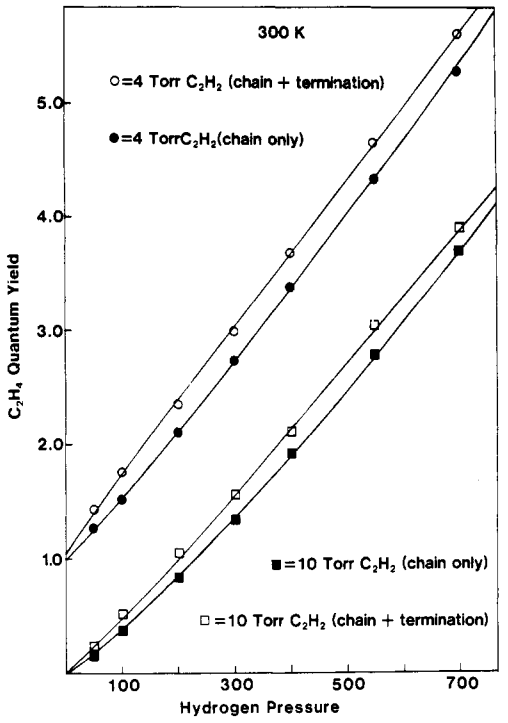

Figure 17. Comparison of the chain formation of C_2H_4 with the chain plus termination yields. The data for $[C_2H_2]$ at 4 Torr have been displaced by one quantum yield unit for clarity (all data 300 K).

derived radical concentrations at the centroid as a function of $[H_2]$, and they are given in Figures 14 and 15.

A similar procedure was applied at 400 K, varying γ to fit the C_2H_4 yields of Figure 7. The required value of γ is 0.78; the quantity has to be finite at the higher temperature, because with $\gamma = 0$ the maximum possible C_6H_6 quantum yield is 2.0: experimentally, a quantum yield of ~4 is found with $[C_2H_2]$ at 60 Torr, and it is still rising with increasing $[C_2H_2]$ (Figure 7). The experimental yields were measured after prediction from the model, and the two are in excellent agreement.

Model calculations are also compared to experimental quantities in Figures 2, 3, 5, and 6; in general, the agreement is good.

Discussion

The model can be applied to predict the dependence of the product yields on the light intensity, by scaling T with the square root of the excitation rates. Experimentally, product ratios were measured with and without interposition of a neutral filter having a 0.26 transmission; these quantities were taken to be of the form 0.26^n, and a set of n for C_2H_4 and C_4H_6 yields are given in Figure 16, for the $[C_2H_2] = 10$ Torr results at 300 K. Small errors in the ratios cause significant changes of n and scatter of the data points, but the trend to increasing n with decreasing $[H_2]$ is found, as predicted by the model. For the C_2H_4 product at 300 K, the exponents do increase significantly above the model calculations, for small $[H_2]$. This behavior is not found at 400 K, where the n agree comparatively well with the model over the full $[H_2]$ range. At 300 K, the high n arise because C_2H_4 is produced in termination reactions of C_2H_3.

To explore further the termination products at 300 K, a series of experiments were undertaken with gas mixtures typically of the composition $[C_2H_2] = 2$ Torr, $[H_2] = 10$ Torr, and $[N_2] = 400$ Torr; recorded C_2H_4 quantum yields are 0.29 with full light and 0.28 with the neutral filter. The model was then applied to predict what fraction of C_2H_4 results from reaction 1, what fraction of C_2H_3 comprises the total radical concentration, and what fraction of C_2H_3 terminates) mutually. After subtracting the chain component ($\Phi = 0.052$ with the full light) from the observed quantum yields and scaling with $((R)_{total})^2/[C_2H_3]^2 = 1.52$, we found the yield of C_2H_4 per mutual termination by two C_2H_3 radicals to be ~0.37. We cannot make a correction for the fraction of $Hg(^3P_1)$ quenched by C_2H_2 because the subsequent reactions are not known. The yields of C_4H_6 produced in the same reaction appear to be quite small, very roughly 0.12.

The C_2H_4 quantum yields by termination are important in relation to the apparently linear variation of $[C_2H_4]$ with $[H_2]$ at 300 K, illustrated in Figures 2 and 3; the model predicts a greater than first order dependence on $[H_2]$, and the discrepancy posed a difficulty in the early stages of this research. However, it is now clear that the effect is due to supplementation of chain production of C_2H_4 with its formation by termination. In Figure 17, the chain and chain plus termination yields have been computed from the model over the range of $[H_2]$. The termination component is taken to be $0.37([R]_{total})^2/[C_2H_3]^2$. The form of the variation of the sum with $[H_2]$ is in accord with experiment.

Several other investigations of the termination products of C_2H_3 have been published.[20-22] Most of the systems are either as complex as the present one or more so. Termination products have not been separated from those produced by the chain steps.

Acknowledgment. This research is supported by the United Kingdom Atomic Energy Authority. We are grateful to Dr. P. A. V. Johnson for informative discussions and to Dr. C. F. Melius for communication of unpublished results.

Registry No. H, 12385-13-6; C_2H_2, 74-86-2; C_2H_3, 2669-89-8; H_2, 1333-74-0.

(20) L. Szirovicza, *Int. J. Chem. Kinet.*, **17**, 117 (1985).
(21) N. A. Weir, *J. Chem. Soc.*, 6870 (1965).
(22) A. G. Sherwood and H. E. Gunning, *J. Phys. Chem.*, **69**, 2323 (1965).